Jet Algorithms and the Underlying Event

Rick Field and David Stuart

Contribution to the Run II Workshop on QCD and Weak Boson Physics
February 1, 2000

Abstract. We examine and compare a variety of jet algorithms applied to charged particles ($P_T > 0.5\,\mathrm{GeV}$, $|\eta| < 1$) in proton-antiproton collisions at $1.8\,\mathrm{TeV}$. In particular, we study how the jet algorithm affects the "size" and "impurity" of the leading charged particle jet. The "impurity" of a jet is the fraction of jet particles or fraction of the scalar P_T sum arising from the underlying event. Any jet algorithm to be used in collider physics must be judged in the context of the collider environment (*i.e.,* messy underlying event). From this point of view our analysis favors the k_T algorithm approach over the midpoint method.

I INTRODUCTION

In a separate analysis presented at this workshop [1] we examined the growth and development of "charged particle jets" produced in proton-antiproton collisions at $1.8\,\mathrm{TeV}$. In addition, we carefully studied the growth and structure of the "underlying event" in hard scattering processes. A "hard scattering" event, like that illustrated in Fig. 1 consists of large transverse momentum outgoing hadrons that originate from the large transverse momentum partons (*i.e.,* outgoing hard scattering "jets") and also hadrons that originate from the break-up of the proton and antiproton (*i.e.,* the "beam-beam remnants"). The "underlying event" is an interesting object that is not very well understood. In addition to beam-beam remnants, it may contain hadrons resulting from initial-state radiation.

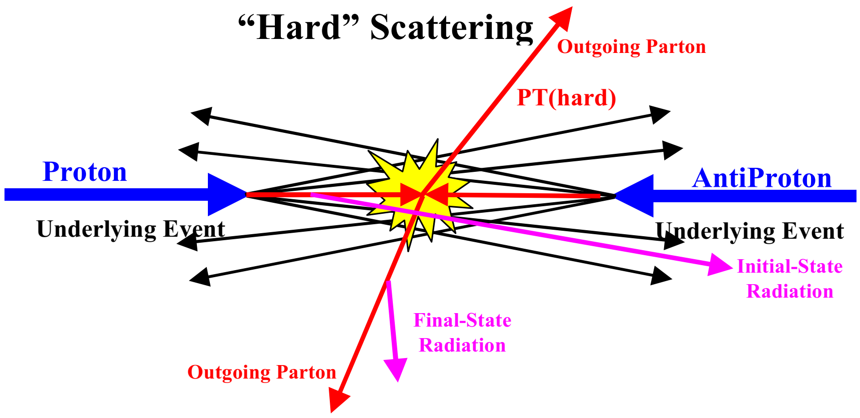

FIGURE 1. Illustration of a proton-antiproton collision in which a "hard" 2-to-2 parton scattering with transverse momentum, $P_T(\mathrm{hard})$, has occurred. The resulting event contains particles that originate from the two outgoing partons (plus final-state radiation) and particles that come from the breakup of the proton and antiproton (*i.e.,* "beam-beam remnants"). The "underlying event" consists of the beam-beam remnants plus initial-state radiation.

In our analysis, we used a very simple jet algorithm to define charged particle "jets" and examined the evolution of these "jets" from $P_T(\mathrm{jet}) = 0.5$ to $50\,\mathrm{GeV}$. As illustrated in Fig. 2, we defined "jets" as "circular regions" ($R = 0.7$) in η-ϕ space and used an algorithm that consisted of first defining "seeds" as all charged particles with $P_T > 0.5\,\mathrm{GeV}$ and $|\eta| < 1$. The seeds were then ordered according to their transverse momentum. We then started with the highest P_T seed and included in the "jet" all particles within the "radius" $R = 0.7$ around the seed. The next highest P_T seed (*not already included in a "jet"*) was then examined and we added to that "jet" all particles (*not already included in a "jet"*) within $R = 0.7$ of that seed. The process was continued until all particles were in a "jet". This simple algorithm worked very well even for jets consisting of only a few charged particles. At low transverse momentum, a single high P_T particle is a good indication of a "jet".

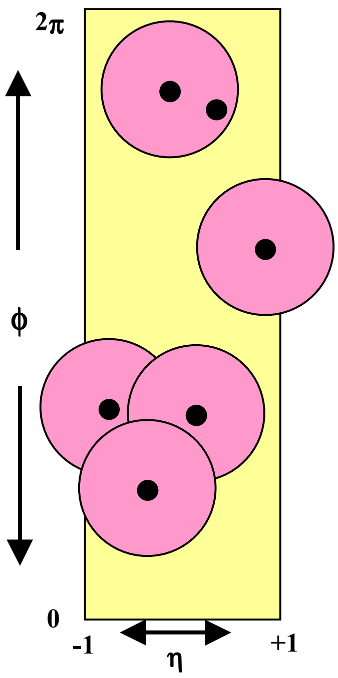

FIGURE 2. Illustration of an event with six charged particles ($P_T > 0.5\,\mathrm{GeV}$ and $|\eta| < 1$) and five charged "jets" (circular regions in η-ϕ space with $R = 0.7$).

Our simple algorithm is, however, not theoretically favored since if applied at the parton level it is not infrared safe. In addition, it is not standard since the initial ordering of the seeds was done according the transverse momentum of the seed rather than according to the *scalar* P_T sum of particles within $R = 0.7$ of the seeds. In this analysis we will examine and compare a variety of jet algorithms. In particular, we study how the jet algorithm affects the "impurity" of the leading jet. Jets defined in hadron-hadron collisions always contain particles from the underlying event. The "impurity" of a jet is the fraction of jet particles arising from the underlying event. In comparing the merits of the various jet algorithms for use at a hadron- hadron collider one should also consider the "impurity" of the leading jet. The goal is to find the particles that arise from the outgoing "hard scattering" partons.

In Section II we discuss the five jet algorithms considered in this analysis. In Section III, we examine the evolution of charged particle "jets" from $P_T(\mathrm{jet}) = 0.5$ to $50\,\mathrm{GeV}$ and we compare the leading charged particle "jet" resulting from five jet algorithms applied to QCD "hard scattering" events generated by ISAJET 7.32. The jet algorithms are applied to the same set of ISAJET events. Since ISAJET employs "independent fragmentation" it is possible to trace particles back to their origin and to examine the contributions from the underlying event (*beam-beam remnants plus initial-state radiation*). Section IV is reserved for summary and conclusions.

II JET ALGORITHMS

In this section, we list the various jet algorithms considered in this analysis. The algorithms are applied to charged particles with $P_T > 0.5\,\mathrm{GeV}$ and $|\eta| < 1$. The resulting "jets" contain charged particles from the underlying event as well as particles which originate from the fragmentation of high P_T outgoing partons (see Fig. 1).

A Jet Definition 0 (seed P_T order)

Jet definition 0 is the simple algorithm we used in our previous analysis [1]. Jets are defined as circular regions in η-ϕ space with "radius" given by, $R = \sqrt{(\Delta\eta)^2 + (\Delta\phi)^2}$. The "seeds" are all charged particles with $P_T > 0.5\,\mathrm{GeV}$ and $|\eta| < 1$ and the algorithm is as follows:

- Order all seeds according to their P_T.
- Start with the highest P_T seed and include in the "jet" all particles within the "radius" $R = 0.7$ seed.
- Go to the next highest P_T seed (*not already included in a "jet"*) and add to the "jet" all particles (*not already included in a "jet"*) within $R = 0.7$.
- Continue until all particles are in a "jet".

We consider all charged particles ($P_T > 0.5\,\mathrm{GeV}$ and $|\eta| < 1$) and we allow the jet radius to extend outside $|\eta| < 1$. Fig. 2 illustrates an event with six charged particles and five jets. We define the transverse momentum of the "jet" to be the *scalar* P_T sum of all the particles within the "jet" (*i.e.,* it is simply the *scalar* P_T sum within the circular region).

B Jet Definition 10 (seed PT_{sum} order)

Jet definition 10 is very similar to definition 0 except that the seeds are ordered according to the *scalar* P_T sum within R = 0.7 of the seed (*double counting of particles is allowed*). The "seeds" are all charged particles with $P_T > 0.5\,\mathrm{GeV}$ and $|\eta| < 1$ and the algorithm is as follows:

- Order all seeds according to the *scalar* P_T sum of all charged particles within $R = 0.7$ of the seed.
- Start with the highest PT_{sum} seed and include in the "jet" all particles within the "radius" $R = 0.7$ of the seed.
- Go to the next highest PT_{sum} seed (*not already included in a "jet"*) and add to the "jet" all particles (*not already included in a "jet"*) within $R = 0.7$.
- Continue until all particles are in a "jet".

All charged particles ($P_T > 0.5\,\mathrm{GeV}$ and $|\eta| < 1$) are considered and we allow the jet radius to extend outside $|\eta| < 1$. We define the transverse momentum of the "jet" to be the *scalar* P_T sum of all the particles within the "jet" (*i.e.,* it is simply the *scalar* P_T sum within the circular region).

C Jet Definition 12A and 12B (midpoint algorithm)

Jet definition 12 is the same as definition 10 except that one adds additional "pseudo-seeds" corresponding to the midpoints of certain seed pairs. In version 12A we include the midpoints of all seed pairs (*unweighted*). In version 12B we include the pseudo-seed only if the distance η-ϕ space between the seed pair, ΔR, satisfies $0.7 < \Delta R < 1.4$ and the midpoint is determined by P_T weighting. The seeds and pseudo-seeds are then ordered according the *scalar* P_T sum of particles within $R = 0.7$ of the seed or pseudo-seed and one proceeds as in definition 10.

D Jet Definition 20 (k_T algorithm)

Jet definition 0 and 10 differ only in the order in which the seeds are processed. The k_T algorithm is designed to be order independent. Again, the initial "seeds" are all charged particles with $P_T > 0.5\,\mathrm{GeV}$ and $|\eta| < 1$. At the start each seed is labeled a "prejet" and a "measure", M, is defined for each prejet and pair of prejets as follows:

$$M(\text{single prejet}) = P_T^2$$
$$M(\text{prejet pair}) = min(P_{T1}^2, P_{T2}^2)((\eta_2 - \eta 1)^2 + (\phi_2 - \phi_1)^2)/R^2$$

where we define the P_T of a prejet to be the *scalar* P_T sum of the particles within the prejet and we take the radius $R = 0.7$. The algorithm then proceeds as follows:

- Compute the "measure", M, of all prejets and all pairs of prejets.
- Find the prejet or pair of prejets with the smallest "measure", M_{min}.
- If M_{min} arises from a single prejet then promote it to a "jet" and remove its particles from consideration.
- If M_{min} arises from a pair of prejets then combine the pair into a new prejet and recompute M for all prejets and pairs of prejets.
- Continue until all prejets have been promoted to "jets".

The five jet algorithms considered in this analysis are summarized in Table 1.

TABLE 1. Jet algorithms considered in this analysis. In all cases, we use the cone radius $R = 0.7$ and define the transverse momentum of a "jet" to be the *scalar* P_T sum of the particles within the jet. Also, we use pseudo-rapidity rather than true rapidity.

ID	Seeds	Order	Comment
0	Charged Particles ($P_T > 0.5\,\mathrm{GeV}$ and $\lvert\eta\rvert < 1$)	P_T seed	Simple algorithm used in Ref. [1]
10	Charged Particles ($P_T > 0.5\,\mathrm{GeV}$ and $\lvert\eta\rvert < 1$)	PT_{sum} ($R = 0.7$)	Same as ID=0 but different order
12A	Charged Particles ($P_T > 0.5\,\mathrm{GeV}$ and $\lvert\eta\rvert < 1$) plus "pseudo-seeds"	PT_{sum} ($R = 0.7$)	Midpoint Algorithm: all midpoints included (unweighted)
12B	Charged Particles ($P_T > 0.5\,\mathrm{GeV}$ and $\lvert\eta\rvert < 1$) plus "pseudo-seeds"	PT_{sum} ($R = 0.7$)	Midpoint Algorithm: pseudo-seeds $0.7 < \Delta R < 1.4$ (P_T weighted)
20	Charged Particles ($P_T > 0.5\,\mathrm{GeV}$ and $\lvert\eta\rvert < 1$)	none	k_T Algorithm: PT_{sum} and η

E Other Variations (*vector* vs *scalar* P_T, y vs η)

Once one has defined the particles within a given "jet", one can plot either the *scalar* P_T sum of particles within the jet or the vector transverse momentum (*i.e.,* transverse component of the vector sum of the momentum of all the particles within the jet). The *scalar* P_T sum is always greater than or equal to the vector P_T, with the difference being related to the transverse mass of the jet. In Ref. [1] we plotted everything in terms of the *scalar* P_T sum and our jet definition did not depend on this choice. Jet definition 0 is the same regardless of whether one defines the transverse momentum of a jet to the scalar or vector P_T. However, the other algorithms in Table 1 do depend on the choice of using scalar or vector jet P_T. For example, the order the seeds are processed in definition 10 might depend on whether one chooses scalar or vector P_T and the "measure", M, in the k_T algorithm changes slightly if one uses vector instead of scalar P_T. We will examine the difference between scalar and vector P_T in a future analysis. Here we consider only the *scalar* P_T choice.

In general one would prefer a jet algorithm that is boost invariant, which means that one should use the true rapidity, y, rather than the pseudo-rapidity, η, to define the cone radius, R. Similarly one might want to use y instead of η in defining the "measure" M in the k_T algorithm. In the data we do not know the mass of the charged particle "seeds", but we could assign all seed masses to be zero (or a pion mass) and use y instead of η. We will study this in a future analysis. Here we will continue to use the pseudo-rapidity.

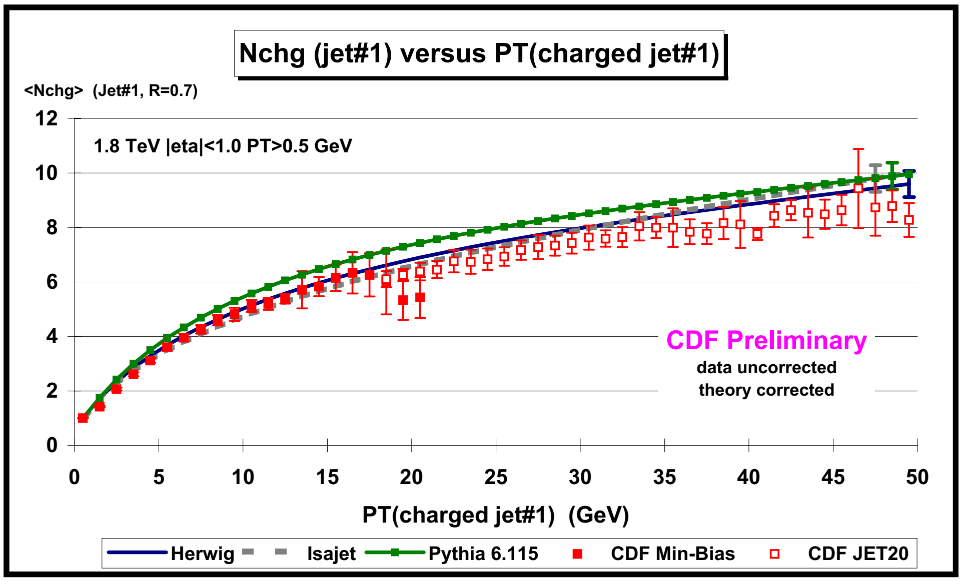

FIGURE 3. Plot shows the average number of charged particles ($P_T > 0.5$ GeV and $|\eta| < 1$) within the leading charged jet (definition 0, $R = 0.7$) as a function of the P_T of the leading charged jet. The solid (open) points are Min-Bias (JET20) data. The errors on the (*uncorrected*) data include both statistical and correlated systematic uncertainties. The QCD "hard scattering" theory curves (HERWIG 5.9, ISAJET 7.32, PYTHIA 6.115) are corrected for the track finding efficiency and have an error (*statistical plus systematic*) of around 5%.

III THE EVOLUTION OF CHARGE PARTICLE "JETS" FROM 0.5 TO 50 GEV

A Charged Jet Multiplicity versus P_T(jet#1)

Fig. 3 shows the average number of charged particles ($P_T > 0.5$ GeV and $|\eta| < 1$) within jet#1 (*leading charged jet*) as a function of P_T(jet#1) using jet definition 0 from Ref. [1]. The solid points are CDF Min-Bias data and the open points are the CDF JET20 data. The JET20 data connect smoothly to the Min-Bias data and allows us to study observables over the range $0.5 < P_T(\text{jet}\#1) < 50$ GeV. There is a small overlap region where the Min-Bias and JET20 data agree. The errors on the data include both statistical and correlated systematic uncertainties. Fig. 3 shows a sharp rise in the leading charged jet multiplicity at low P_T(jet#1) and then a flattening out and a gradual rise at high P_T(jet#1). The data are compared with the QCD "hard scattering" Monte-Carlo predictions of HERWIG 5.9 [2], ISAJET 7.32 [3], and PYTHIA 6.115 [4]. The theory curves are corrected for the track finding efficiency and have an error (*statistical plus systematic*) of around 5%. We, of course, used the same jet definition for both the data and the theory and the QCD "hard scattering" models have $P_T(\text{hard}) > 3$ GeV.

Our philosophy in comparing the theory with data is to select a region where the data is very "clean". The CDF track finding efficiency can vary substantially for very low P_T tracks and in dense high P_T jets. To avoid this we have considered only the region $P_T > 0.5$ GeV and $|\eta| < 1$) where the efficiency is high and stable (estimated to be 92% efficient) and we restrict ourselves to jets less than 50 GeV. The data are uncorrected. Instead the theoretical Monte-Carlo predictions are corrected for the track finding efficiency and have an error (*statistical plus systematic*) of about 5%. The errors on the (uncorrected) data include both statistical and correlated systematic uncertainties.

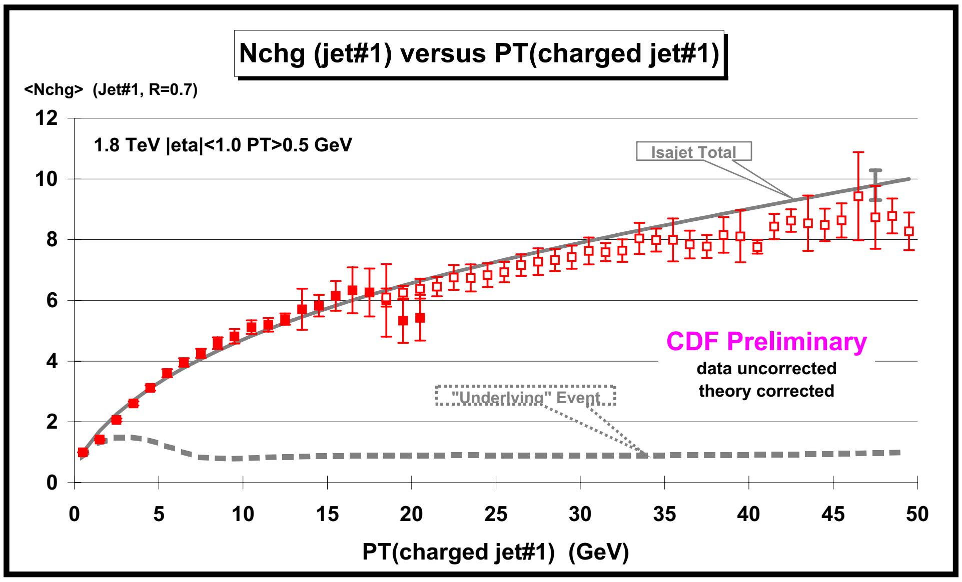

FIGURE 4. Data from Fig. 3 on the average number of charged particles ($P_T > 0.5\,\mathrm{GeV}$, $|\eta| < 1$) within the leading charged jet (definition 0, $R = 0.7$) as a function of the P_T of the leading charged jet compared with the QCD "hard scatteriing" predictions of ISAJET 7.32. Also shown is the contribution from the underlying event (*beam- beam remnants plus initial-state radiation*) predicted by ISAJET (see Fig. 1). The errors on the (*uncorrected*) data include both statistical and correlated systematic uncertainties. The theory curves are corrected for the track finding efficiency and have an error (*statistical plus systematic*) of around 5%.

Fig. 4 is the same as Fig. 3 except here we show only the predictions from ISAJET 7.32. Since ISAJET employs "independent fragmentation" it is possible to trace particles back to their origin and divide them into three categories: particles that arise from the break-up of the beam and target (*beam-beam remnants*), particles that arise from initial-state radiation, and particles that result from the outgoing hard scattering jets plus final-state radiation. The "hard scattering component" consists of the particles that arise from the outgoing hard scattering jets plus initial and final-state radiation (*sum of the last two categories*). Particles from the first two categories (*beam-beam remnants plus initial-state radiation*) are normally what is referred to as the underlying event (see Fig. 1). Fig. 4 shows the contribution of the underlying event (*beam-beam remnants plus initial-state radiation*) to the leading charged particle jet multiplicity for jet definition 0. When one constructs jets in hadron-hadron collisions one cannot avoid contamination from the underlying event.

Fig. 5 shows the average number of charged particles within the leading charged jet as a function of the P_T of the leading charged jet resulting from the five jet algorithms in Table 1 applied to QCD "hard scattering" events generated by ISAJET 7.32. Note that the five jet algorithms are applied to the *same* set of ISAJET events. Also shown in Fig. 5 are the "true" particles belonging to the leading jet (*ISAJET True*) plotted versus the "true" jet P_T (*scalar* P_T sum). As discussed earlier, since ISAJET uses "independent fragmentation" it is possible to trace particles back to their origin and to construct the "true" outgoing jets. The leading jets constructed from the five jet algorithms with $R = 0.7$ have a larger multiplicity of charged particles than the "true" jets due to contamination from the underlying event.

B Charged Jet "Size" versus P_T(jet#1)

Although the charged particle jets are defined with $R = 0.7$, this is not the "size" of the jet. The "size" of a jet can be defined in two ways; size according to particle number, and size according to transverse momentum. The first corresponds to the radius in η-ϕ space that contains 80% of the charged particles in the jet and the second corresponds to the radius in η-ϕ space that contains 80% of the jet transverse momentum. The data on the average "jet size" of the leading charged particle jet are compared with the QCD "hard scattering" Monte-Carlo predictions of HERWIG 5.9, ISAJET 7.32, and PYTHIA 6.115 in Fig. 6 for jet definition 0. Fig. 6 clearly illustrate the "hot core" of jets. The radius containing 80% of the transverse momentum is smaller than the

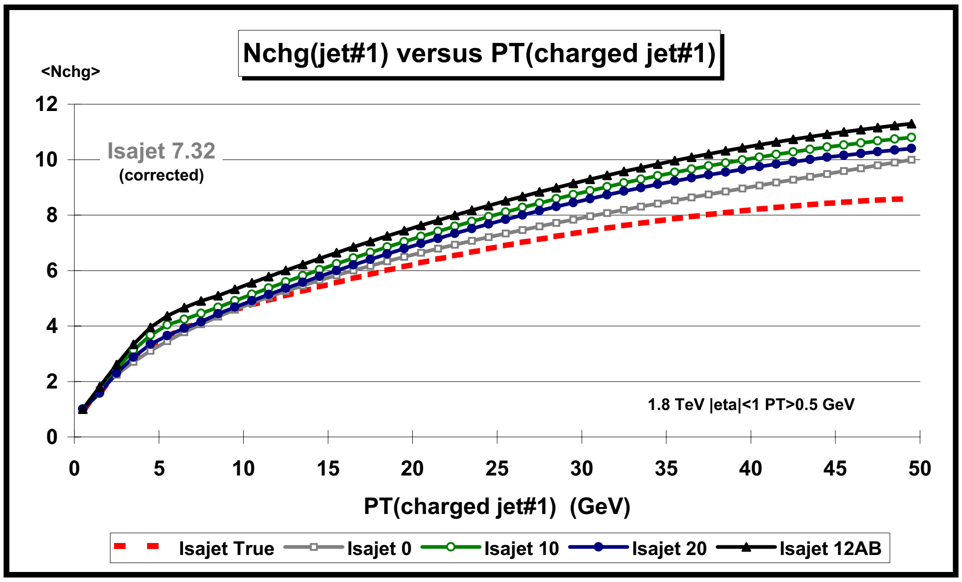

FIGURE 5. Shows the average number of charged particles ($P_T > 0.5\,\mathrm{GeV}$, $|\eta| < 1$) within the leading charged jet as a function of the P_T of the leading charged jet resulting from the five jet algorithms in Table 1 applied to QCD "hard scattering" events generated by ISAJT 7.32. Note that the five jet algorithms are applied to the *same* set of Isajet events. Also shown are the "true" particles belonging to the leading jet (*Isajet True*) plotted versus the "true" jet P_T. The theory curves are corrected for the track finding efficiency and have an error (*statistical plus systematic*) of around 5%.

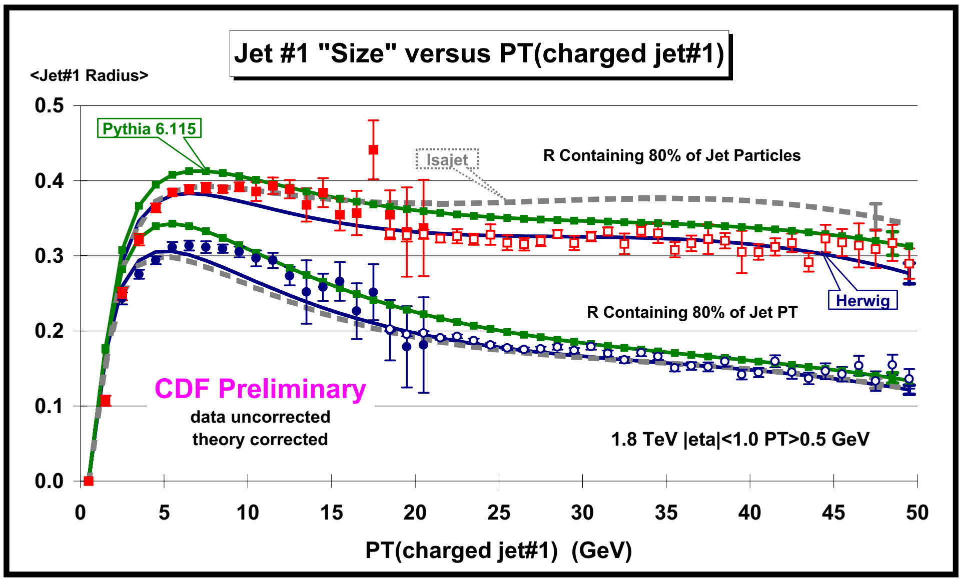

FIGURE 6. Plot shows the average radius in η-ϕ space containing 80% of the charged particles (and 80% of the charged P_T) as a function of the transverse momentum of the leading charged jet (definition 0). The errors on the (*uncorrected*) data include both statistical and correlated systematic uncertainties. The QCD "hard scattering" theory curves (HERWIG 5.9, ISAJET 7.32, PYTHIA 6.115) are corrected for the track finding efficiency and have an error (*statistical plus systematic*) of around 5%.

radius that contains 80% of the particles. Furthermore, the radius containing 80% of the transverse momentum decreases as the overall transverse momentum of the jet increases due to limited momentum perpendicular to the jet direction.

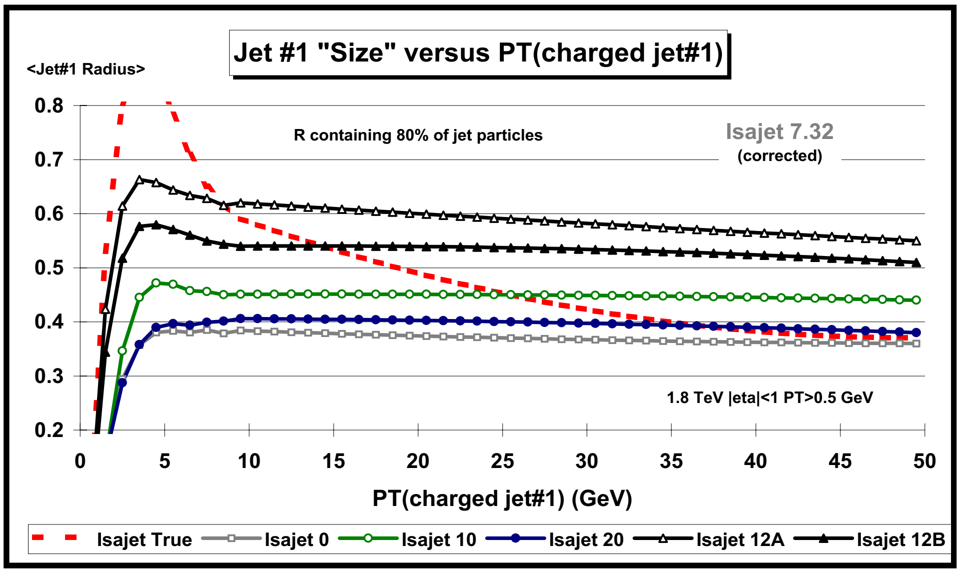

FIGURE 7. Plot shows the average radius in η-ϕ space containing 80% of the charged particles as a function of the transverse momentum of the leading charged jet resulting from the five jet algorithms in Table 1 applied to QCD "hard scattering" events generated by ISAJET 7.32. Note that the five jet algorithms are applied to the *same* set of Isajet events. Also shown are the "true" particles belonging to the leading jet (*Isajet True*) plotted versus the "true" jet P_T. The theory curves are corrected for the track finding efficiency and have an error (*statistical plus systematic*) of around 5%.

Fig. 7 and Fig. 8 show the average radius in η-ϕ space containing 80% of the charged particles and the average radius in η-ϕ space containing 80% of the charged P_T sum, respectively, as a function of the transverse momentum of the leading charged jet ($R = 0.7$) resulting from the five jet algorithms in Table 1 applied to QCD "hard scattering" events generated by ISAJET 7.32. The five jet algorithms are applied to the *same* set of ISAJET events. Also shown are the "true" particles belonging to the leading jet (*ISAJET True*) plotted versus the "true" jet P_T. Clearly the algorithms do not always select the same leading jet! The midpoint algorithms (definition 12A and 12B) produces "fatter" leading jets, on the average, than does the k_T algorithm (definition 20). Furthermore the k_T algorithm (definition 20) produced results that are very similar to the simple algorithm we used in Ref. [1] (definition 0).

C Charged Jet "Impurity" versus P_T(jet#1)

It is interesting to see how the jet algorithm affects the contamination of the leading charged particle "jet" from the underlying event. Fig. 9 shows the contribution to the number of charged particles within the leading charged jet from the underlying event (*beam-beam remnants plus initial-state radiation*) resulting from the five jet algorithms in Table 1 applied to QCD "hard scattering" events generated by ISAJET 7.32. As before, the five jet algorithms are applied to the same set of ISAJET events. Fig. 10 shows the fraction of charged particles within the leading charged jet arising from the underlying event (beam-beam remnants plus initial-state radiation) resulting from the five jet algorithms in Table 1 applied to QCD "hard scattering" events generated by ISAJET 7.32.

Fig. 11 shows the contribution to charged particle *scalar* P_T sum within the leading charged jet arising from the underlying event (*beam-beam remnants plus initial-state radiation*) resulting from the five jet algorithms in Table 1 applied to QCD "hard scattering" events generated by ISAJET 7.32. As always, the five jet algorithms are applied to the same set of ISAJET events. Fig. 12 shows the fraction of charged particle *scalar* P_T sum within the leading charged jet arising from the underlying event (*beam-beam remnants plus initial-state radiation*). The leading jets for the midpoint algorithms (definition 12A and 12B) are "fatter" because

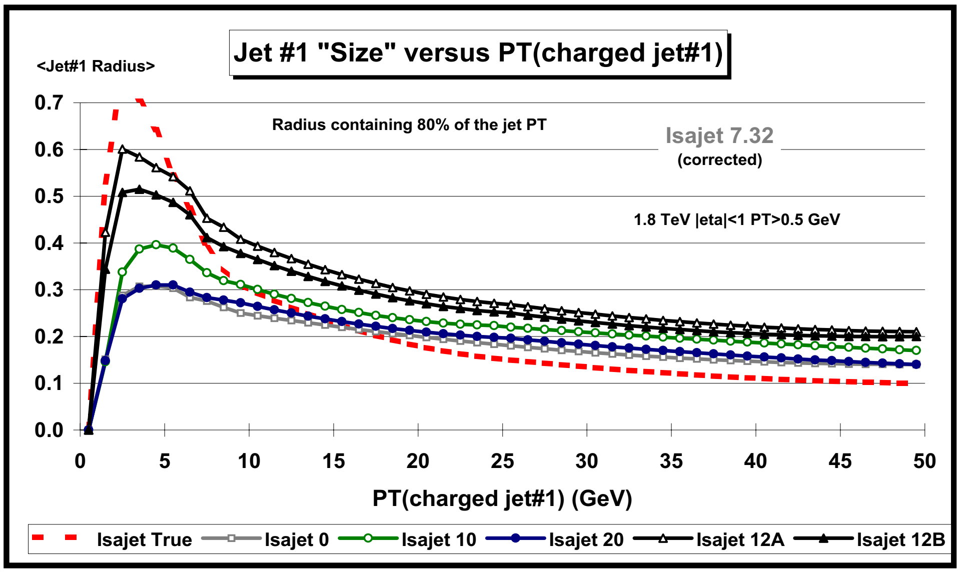

FIGURE 8. Plot shows the average radius in η-ϕ space containing 80% of the charged particle *scalar* P_T sum as a function of the transverse momentum of the leading charged jet resulting from the five jet algorithms in Table 1 applied to QCD "hard scattering" events generated by ISAJET 7.32. Note that the five jet algorithms are applied to the *same* set of ISAJET events. Also shown are the "true" particles belonging to the leading jet (*Isajet True*) plotted versus the "true" jet P_T. The theory curves are corrected for the track finding efficiency and have an error (*statistical plus systematic*) of around 5%.

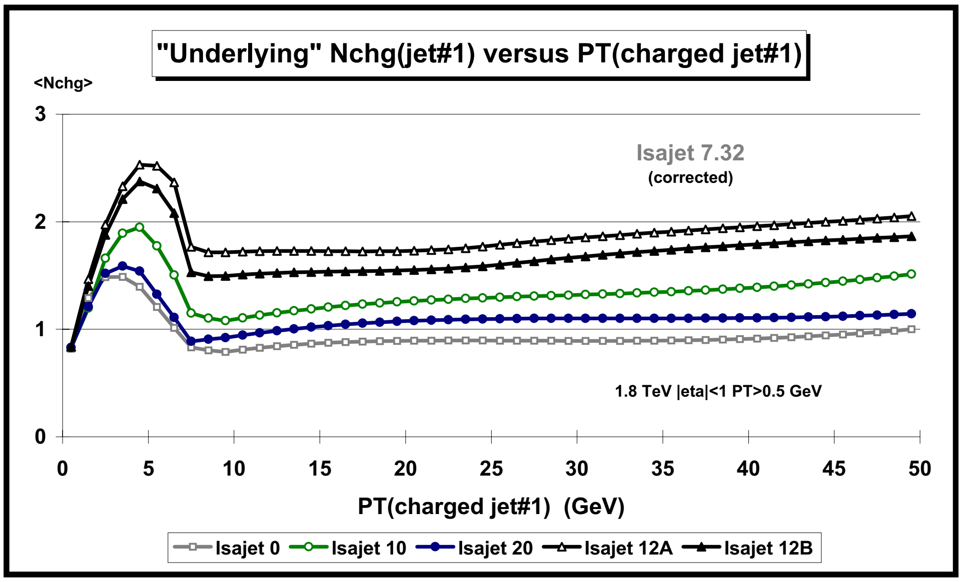

FIGURE 9. Shows the contribution to the number of charged particles ($P_T > 0.5\,\mathrm{GeV}$, $|\eta| < 1$) within the leading charged jet arising from the underlying event (*beam- beam remnants plus initial-state radiation*, see Fig. 1) as a function of the P_T of the leading charged jet resulting from the five jet algorithms in Table 1 applied to QCD "hard scattering" events generated by ISAJET 7.32. Note that the five jet algorithms are applied to the *same* set of ISAJET events. The theory curves are corrected for the track finding efficiency and have an error (*statistical plus systematic*) of around 5%.

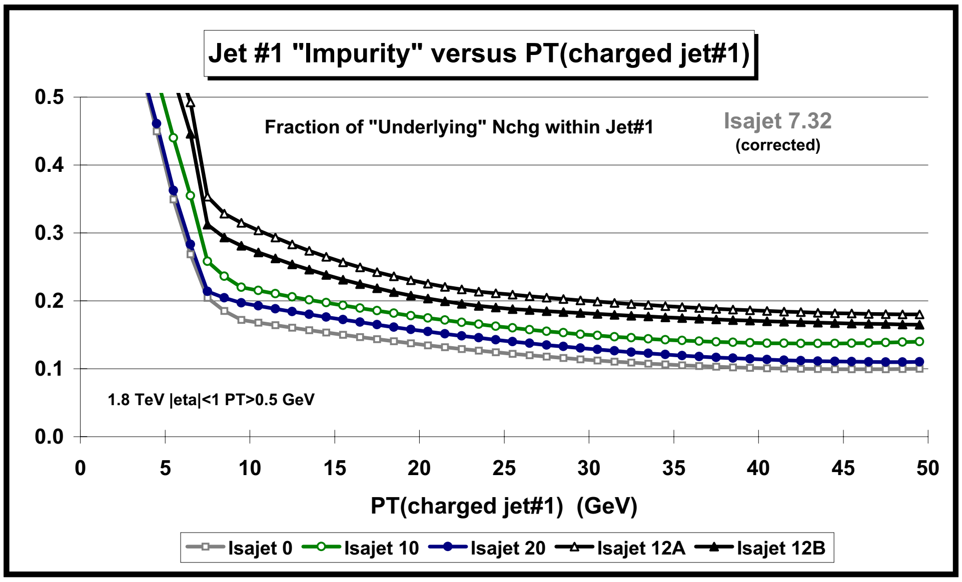

FIGURE 10. Shows the fraction of charged particles ($P_T > 0.5\,\mathrm{GeV}$, $|\eta| < 1$) within the leading charged jet arising from the underlying event (*beam-beam remnants plus initial-state radiation*, see Fig. 1) as a function of the P_T of the leading charged jet resulting from the five jet algorithms in Table 1 applied to QCD "hard scattering" events generated by ISAJET 7.32. Note that the five jet algorithms are applied to the *same* set of ISAJET events. The theory curves are corrected for the track finding efficiency and have an error (*statistical plus systematic*) of around 5%.

they contain a higher fraction of particles arising from the underlying event. In hadron-hadron collisions all jet definitions result in some "impurity". Of the five algorithms considered in this analysis, the k_T algorithm (definition 20) and the simple algorithm we used in Ref. [1] (definition 0) produce leading charged particle jets with the smallest amount of "impurity".

D Charged Jet Cross Section

Of course the leading jet cross section depends on the algorithm used to define a "jet". Fig. 13 shows the charged particle jet cross section, $d\sigma/dP_T(\text{jet\#1})$, ratio resulting from the jet algorithms in Table 1 applied to QCD "hard scattering" events generated by ISAJET 7.32. The ratios correspond to the leading jet cross section from definitions 10, 20, 12A, and 12B divided by the leading jet cross section from definition 0. Since the leading jets for the midpoint algorithm (definition 12A and 12B) are "fatter" (*i.e.,* more transverse momentum), the P_T differential cross section is larger. The k_T algorithm (definition 20) and the simple algorithm we used in Ref. [1] (definition 0) produce almost identical leading jet P_T cross sections.

IV SUMMARY AND CONCLUSIONS

Applying a jet algorithm to hadron-hadron collider events corresponds to selecting a particular observable (*or set of observables*) from the infinite set of possible observables. All observables are infrared and collinear safe at the hadron level. One must study many observables to fully appreciate the complexity of a collider event and, in general, all obsevables that provide pertinent information are equally good. On the other hand, we might demand more from a jet algorithm since we want to use it to infer the structure of underlying QCD "hard scattering" parton-parton subprocess. Because of this we would like jet algorithms to be infrared and collinear safe at the parton level and probably also boost invariant.

Proton-antiproton collider events are not "clean". A "hard scattering" event consists not only of large transverse momentum outgoing hard scattering "jets", but also contains an "underlying event" consisting of hadrons that originate from the break-up of the proton and antiproton (*beam-beam remnants*) and from hadrons arising from initial-state radiation. Although one can try and correct for the contribution to jets from

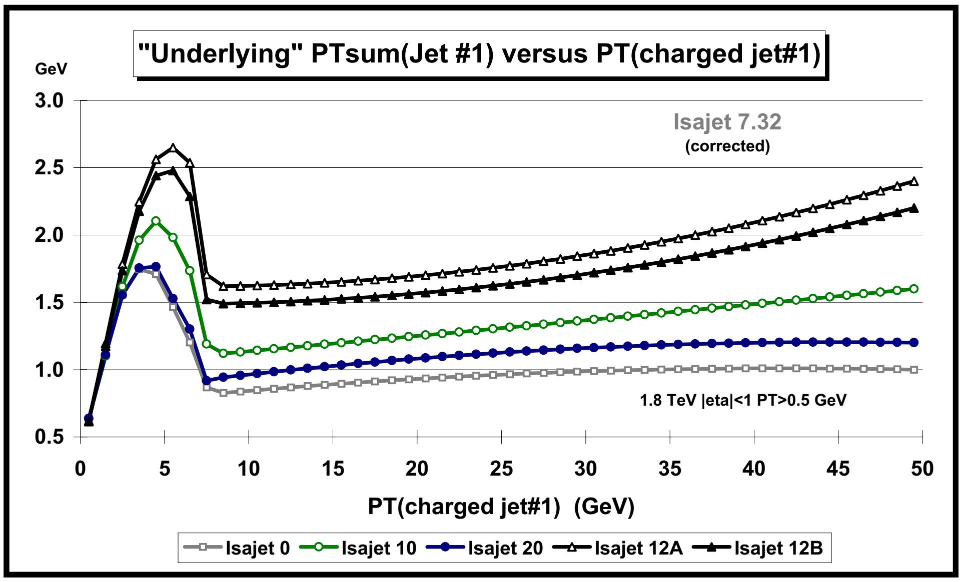

FIGURE 11. Shows the contribution to the charged particle scalar P_T sum ($P_T > 0.5\,\mathrm{GeV}$, $|\eta| < 1$) within the leading charged jet arising from the underlying event (*beam-beam remnants plus initial-state radiation*, see Fig. 1) as a function of the P_T of the leading charged jet resulting from the five jet algorithms in Table 1 applied to QCD "hard scattering" events generated by ISAJET 7.32. Note that the five jet algorithms are applied to the *same* set of ISAJET events. The theory curves are corrected for the track finding efficiency and have an error (*statistical plus systematic*) of around 5%.

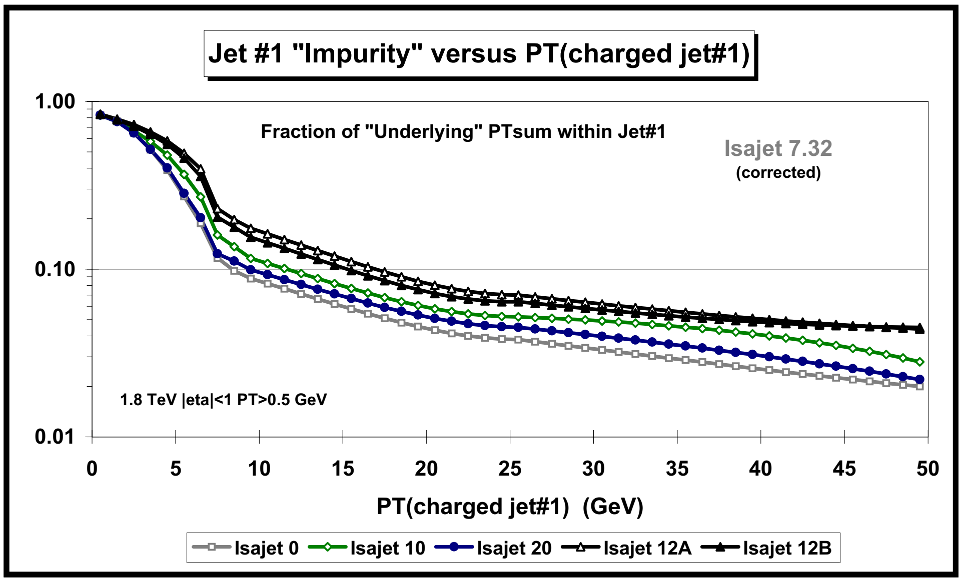

FIGURE 12. Shows the fraction of charged particle scalar P_T sum ($P_T > 0.5\,\mathrm{GeV}$, $|\eta| < 1$) within the leading charged jet arising from the underlying event (*beam- beam remnants plus initial-state radiation*, see Fig. 1) as a function of the P_T of the leading charged jet resulting from the five jet algorithms in Table 1 applied to QCD "hard scattering" events generated by ISAJET 7.32. Note that the five jet algorithms are applied to the *same* set of ISAJET events. The theory curves are corrected for the track finding efficiency and have an error (*statistical plus systematic*) of around 5%.

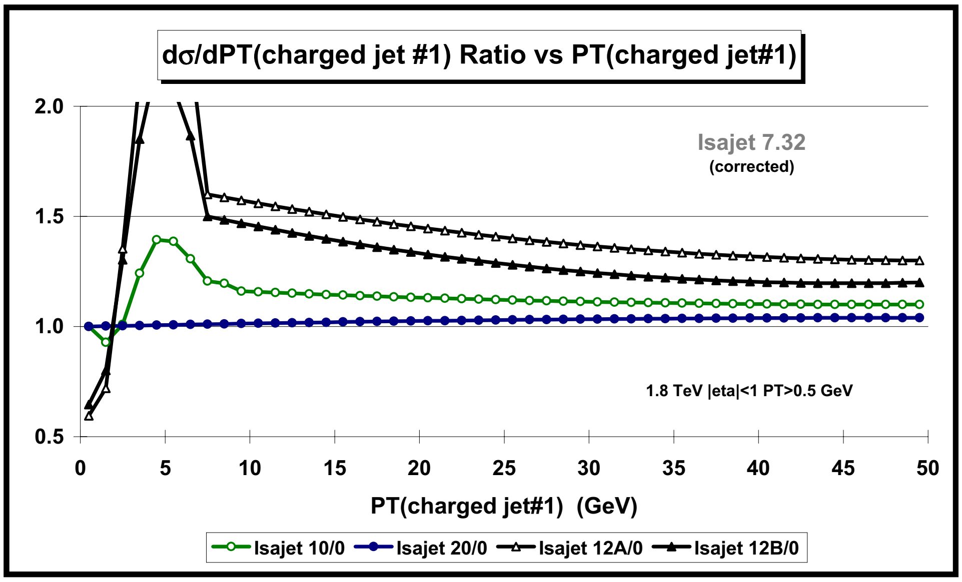

FIGURE 13. Shows the charged particle jet cross section, $d\sigma/dPT(\text{jet}\#1)$, ratio resulting from the jet algorithms in Table 1 applied to QCD "hard scattering" events generated by ISAJET 7.32. The ratios correspond to the leading jet cross sections from definitions 10, 20, 12A, and 12B divided by the leading jet cross section from definition 0. Note that the five jet algorithms are applied to the *same* set of ISAJET events. The theory curves are corrected for the track finding efficiency and have an error (*statistical plus systematic*) of around 5%.

the underlying event, it would seem reasonable to choose a jet algorithm that minimizes the "impurity" of the jets. In hadron-hadron collisions all jet definitions result in some "impurity". Of the five algorithms considered in this analysis, the k_T algorithm (definition 20) and the simple algorithm we used in Ref. [1] (definition 0) produce leading charged particle jets with the smallest amount of "impurity". The k_T algorithm (definition 20) and the simple algorithm (definition 0) produce nearly identical results. However, the k_T algorithm (definition 20) is infrared and collinear safe at the parton level while the simple algorithm (definition 0) is not.

The midpoint algorithms (definition 12A and 12B) preferentially select "fatter" jets than the other algorithms considered. These "fatter" jets have a larger fraction of their multiplicity and a larger fraction of their scalar P_T sum arising from the underlying event than do the jets from the other algorithms. Due to the nature of the mid-point algorithm, one might have expected this to be true.

It is premature to make any definite conclusions. More studies need to be done. It is clear, however, that any jet algorithm to be used in collider physics must be judged in the context of the collider environment (*i.e.,* underlying event). From this point of view our analysis favors the k_T algorithm approach over the midpoint method.

REFERENCES

1. Rick Field and David Stuart, *The Underlying Event in Hard Scattering Processes*, contribution to the Run II Workshop on QCD and Weak Boson Physics, Fermilab, February 1, 2000.
2. G. Marchesini and B. R. Webber, Nucl. Phys **B310**, 461 (1988); I. G. Knowles, Nucl. Phys. **B310**, 571 (1988); S. Catani, G. Marchesini, and B. R. Webber, Nucl. Phys. **B349**, 635 (19991).
3. F. Paige and S. Protopopescu, BNL Report, BNL38034, 1986 (*unpublished*), version 7.32.
4. T. Sjostrand, Phys. Lett. **157B**, 321 (1985); M. Bengtsson, T. Sjostrand, and M. van Zijl, Z. Phys. **C32**, 67 (1986); T. Sjostrand and M. van Zijl, Phys. Rev. **D36**, 2019 (1987).